Journal of the Geological Society, London, Vol. **156,** 1999, pp. 901–916. Printed in Great Britain.

Mesozoic dolerite dykes of the Falkland Islands: petrology, petrogenesis and implications for geochemical provinciality in Gondwanaland low-Ti basaltic rocks

C. MITCHELL[1,3] R. M. ELLAM[2] & K. G. COX[1]*

[1]*Department of Earth Sciences, Oxford University, Parks Road, Oxford OX1 3PR, UK*

[2]*Isotope Geosciences Unit, Scottish Universities Research and Reactor Centre, East Kilbride G75 0QF, UK*

[3]*Present address: Ferryhouse, Holm, Orkney KW17 2RY, UK*

Abstract: The dolerite dykes of central West Falkland provided the first palaeomagnetic evidence of the near-180° rotation of the islands during the break-up of Gondwanaland. Here we present the results of a petrological and geochemical study of those dolerites. Most of the dykes sampled can be assigned to one of two suites named north–south and east–west respectively in recognition of their dominant strike. E–W dykes have compositional affinities with magmas such as the Rooi Rand dolerites of SE Africa whose geochemical characteristics (e.g. $^{87}Sr/^{86}Sr<0.704$) are suggestive of predominantly asthenospheric mantle derivation. N–S dykes, which are the most numerous, resemble the Ferrar magma type of Antarctica and the rare Hangnest and Kraai River magma types of the Karoo. The N–S dykes evolved by assimilation and fractional crystallization (AFC), most likely at crustal levels, leading to initial $^{87}Sr/^{86}Sr=0.708–0.712$, but there is no compelling evidence for initial $^{87}Sr/^{86}Sr<0.708$, perhaps suggesting an enriched lithospheric mantle source. Dykes from Lively Island and Mount Alice appear to be correlatives of other Karoo magma types. All the Falklands dykes are low-Ti in character. However, within this one small area a variety of Karoo low-Ti magma types coexist with the Ferrar magma type of Antarctica. This overlap in space of different low-Ti magma types resembles the situation in Coats Land, Antarctica and enables us to propose an extension of the boundary of the Ferrar province parallel to the subducting margin of Gondwanaland.

Keywords: Falkland Islands, dolerites, Gondwanaland, basalt petrogenesis.

The Falkland Islands represent a small piece of the Gondwanaland jigsaw puzzle. From palaeomagnetic studies and comparisons with the geology of SE Africa (Adie 1952; Mitchell *et al*. 1986; Taylor & Shaw 1989), it is now established that the pre-drift (early Jurassic) position of the islands was adjacent to the South African coast near East London (Fig. 1) and that they have since been rotated through approximately 180°. Hence, the shales of Lafonia in the Falkland Islands represent the southeast corner of the Karoo Basin which is missing in southern Africa (Fig. 1).

This work gives an account of the petrology, geochemistry, and petrogenesis of four suites of dolerite dykes which cut the Palaeozoic sedimentary rocks of the Falkland Islands. The two most important suites (Fig. 2) are termed respectively N–S and E–W in recognition of their predominant strike. These suites are compositionally quite distinct, as illustrated, for example, by MgO–SiO_2 relations (Fig. 3a). In addition, two minor suites called Lively Island (apparently represented by one dyke only) and Mount Alice, are identified. A fifth suite, termed Cape Orford, consists of broadly andesitic rock types, which are highly altered and are not considered in detail in this paper.

An early Jurassic age for the dykes is indicated by the few existing age determinations. Cingolani & Varela (1976) for example, report a K–Ar age of 190 ± 10 Ma, while two Ar–Ar determinations (Musset & Taylor 1994) give 190 ± 4 and 188 ± 2 Ma, and an additional sample gives a less certain estimate, which is only a maximum, of 193 ± 3 Ma. The three Ar–Ar dated samples were taken from the Cape Orford, E–W, and N–S suites respectively. The dates are similar to those from the Karoo Province in southern Africa and the Ferrar basalts of East Antarctica (e.g. Fitch & Miller 1984; Duncan *et al*. 1997) though at the older end of the range. Comparison with the Karoo is not surprising in view of the pre-drift position of the islands. The Lively Island dyke has not been dated, but it is a close compositional analogue to the dominant magma type of the Lesotho Formation of the Karoo (see below). There are no age data for the Mount Alice dykes.

All the dykes sampled are from West Falkland, with the exception of the Lively Island occurrence, which appears to be the only dyke identified in East Falkland (Greenway 1972); sample localities are shown in Fig. 2. The doleritic dykes are wide, typically 10 m, but very poorly exposed, though they are easy to trace in the field because their baked margins (usually quartzite) crop out well. The age relation between the N–S and E–W dykes, although there are many places where they intersect, is unknown because of absence of exposure of the dolerites themselves at the critical localities. The Cape Orford dykes are much narrower, and strike in many different directions.

Petrography

East–west dykes

The samples are mainly porphyritic, with phenocrysts of olivine, plagioclase, and occasionally clinopyroxene, in a fine-grained groundmass of olivine, clinopyroxene, plagioclase, and iron oxides. The phenocrysts are about 1 mm across, and the groundmass has a grain-size of 0.1–0.05 mm. Samples with coarser groundmasses show ophitic to sub-ophitic textures. Olivine phenocrysts (chrysolite) often appear as

*Deceased.

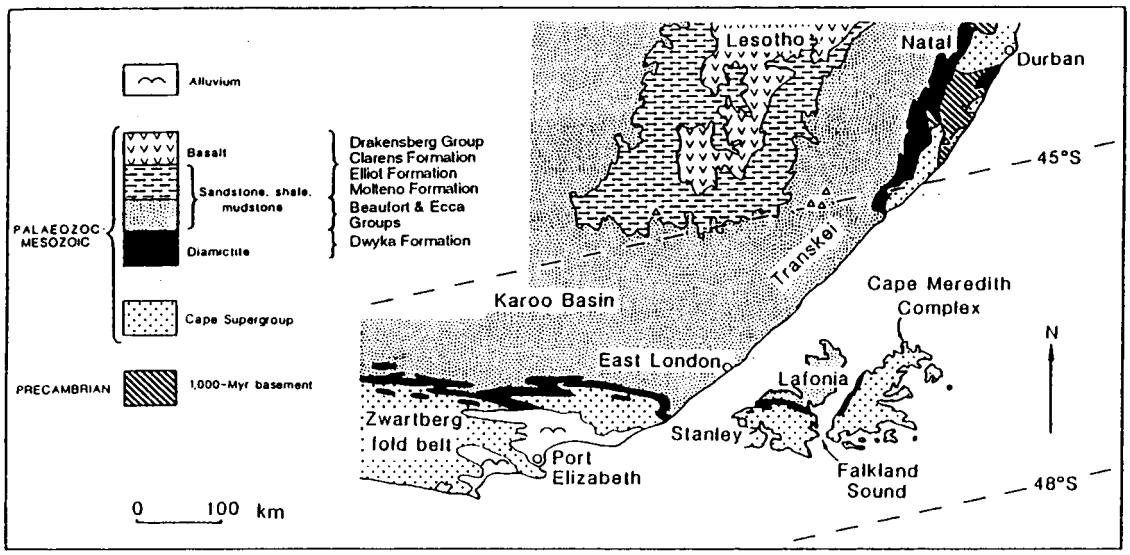

Fig. 1. Geological map showing the Falkland Islands in their pre-drift (early Jurassic) position adjacent to South Africa (after Adie 1952; Mitchell *et al.* 1986).

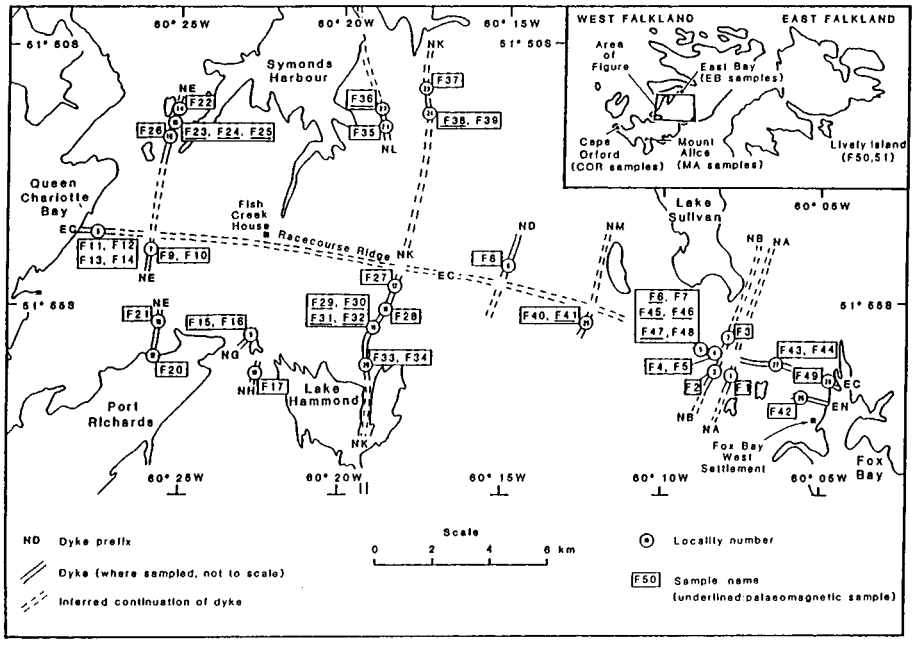

Fig. 2. Sample localities (open circles) and sample numbers. Dykes of N–S suite are labelled NA, NB etc. and of the E–W suite EC and EN. A small E–W dyke termed EJ (not shown) was collected in the vicinity of NH, west of Lake Hammond. In tables of analytical data, the first two letters of the sample name identify the dyke, followed by an F (for Falklands) and the number shown in this figure.

glomeroporphyritic clots up to 3 mm across, while plagioclase phenocrysts (labradorite) usually occur as single crystals. Olivine and plagioclase phenocrysts are present in approximately equal proportions and together typically constitute about 20% of the rock. The samples are mainly very fresh.

North–south dykes

These are coarse-grained (0.5–1 mm) dolerites with an intergranular to sub-ophitic texture. They are similar to a sample described by Brown (1967) which was collected 11 miles NE of Fox Bay (Fig. 2). The essential minerals are plagioclase, clinopyroxene, and orthopyroxene. Clearly identifiable phenocrysts are rare, the texture more commonly being seriate. Orthopyroxenes (bronzite–hypersthene, En_{70-80}) commonly occur as clusters, and are rimmed with clinopyroxene. Modally, the rocks typically consist of labradorite (50%), orthopyroxene and clinopyroxene (20% each). Both augite and pigeonite are present but are difficult to distinguish in thin section. The remainder of the rock (10%) consists of an opaque phase and interstitial material of brownish glass with acicular growths of plagioclase, and dendritic oxides. Quartz is also common, as are well-developed granophyric patches. One sample, NKF34, contains obvious (1 mm) phenocrysts set in a brownish glass containing quench plagioclase and clinopyroxene. The most abundant phenocrysts appear to be altered olivine, and are sometimes rimmed by clinopyroxene. Rare phenocrysts of fresh orthopyroxene are also present. Sample NEF21 contains a small inclusion of strained quartz with veinlets of unstrained quartz, surrounded by a reaction

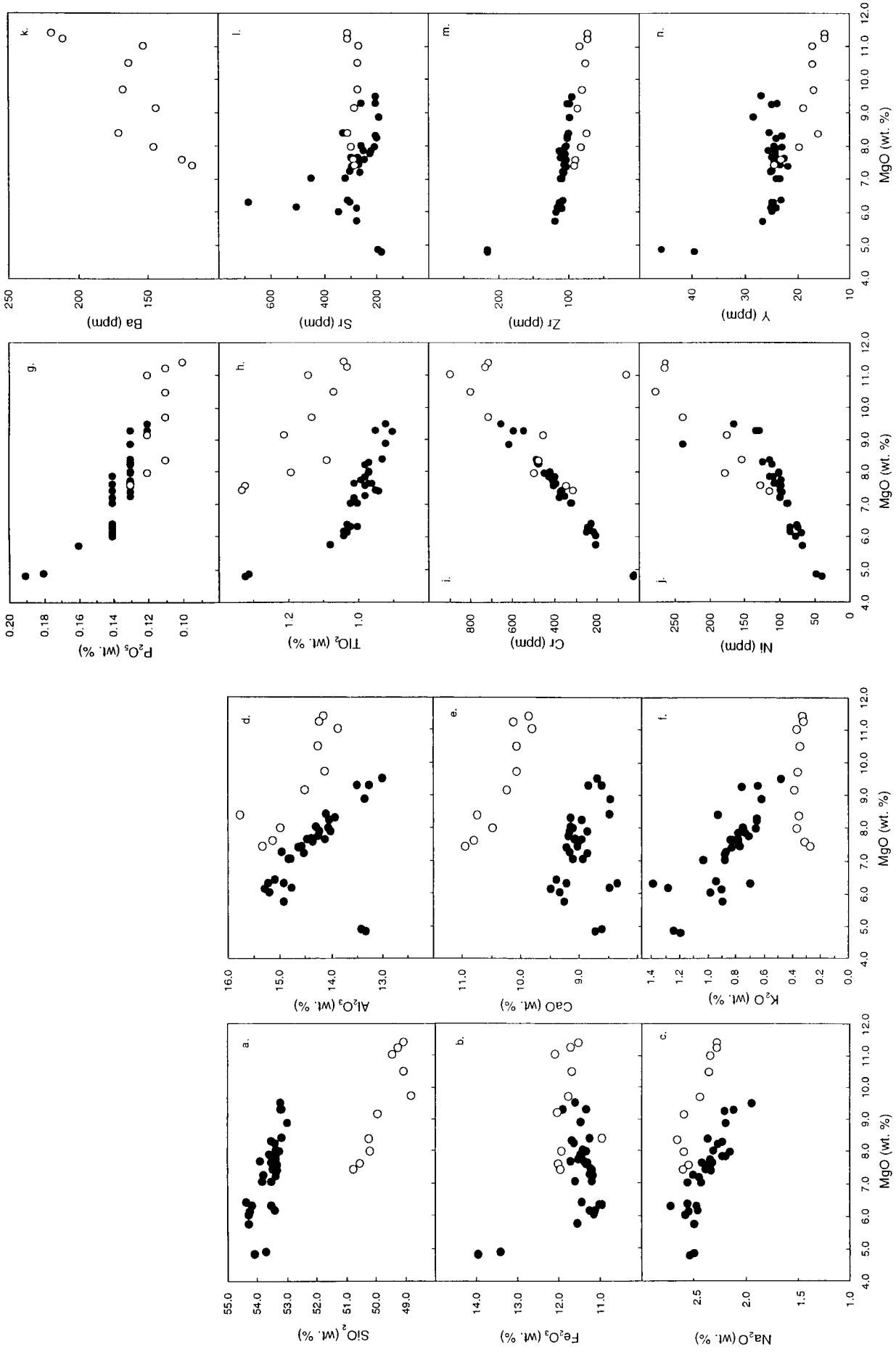

Fig. 3. Variation diagrams for selected major and trace elements v. MgO. Here, and in subsequent figures, open circles are E–W suite, solid dots are N–S suite.

rim. Crustal contamination is inferred from the geochemistry of this suite (see below), but this is the only example found of a possible crustal xenolith.

Lively Island

Samples from this dyke are petrographically broadly similar to those of the N–S suite, but contain much less orthopyroxene.

Mineral compositions

Mineral compositions determined by electron microprobe are given in Table 1. Olivines from the E–W suite yield chrysolite compositions in the restricted range $Fo_{85–82}$. Pyroxenes from the N–S suite have a variety of compositions, including orthopyroxenes in the hypersthene–bronzite range ($En_{70–80}$), and clinopyroxenes which are diopsidic augites ($Wo_{30}En_{50}Fs_{20}$), as well as sub-calcic augites and magnesian pigeonites. Plagioclase compositions from the E–W suite are labradoritic ($An_{62–70}$) while those from the N–S suite are slightly more sodic ($An_{52–65}$). Opaque oxide compositions were determined in two samples from the N–S suite and indicate the presence of both titano-magnetite and ilmenite.

Bulk compositional variation and fractionation trends

East–west dykes

Most of the E–W samples were collected from a single dyke (the Race Course Ridge; EC, see Fig. 2), which is clearly heterogeneous in composition, though whether the heterogeneity represents multiple injection is unknown. In general, the Falklands E–W dykes are fairly primitive (Table 2, Fig. 2), and for most elements show a compositional trend which is consistent with the fractionation of olivine alone, probably with a little chrome spinel (see Fig. 3). The variation diagrams for the major elements show the typical relationships associated with olivine fractionation, and this has been confirmed by mixing calculations, one of which is given in Table 3.

Fractionation of about 12 wt% of olivine from the basic end-member is capable of producing a close major element match to the evolved end-member. Consideration of the relationship between the range of olivine compositions present and the whole rock Fe/Mg ratios, according to the Fe–Mg distribution coefficient of Roeder & Emslie (1970), suggests that the olivines present were in equilibrium with liquids whose compositions were close to those recorded by the whole-rocks; the lack of porphyritic texture is consistent with this observation.

It is notable that, as in several other basaltic suites (e.g. Scarrow & Cox 1995 and references therein), there is a mismatch between the fractionating assemblage deduced from compositional variation (i.e. olivine+Cr-spinel) and the phenocrysts actually present (olivine+plagioclase+occasional clinopyroxene).

The mixing calculation given implies an enrichment factor of 1.14 for incompatible elements, and is broadly consistent with the relatively small enrichments observed (Fig. 3) in Ti, Na, P, Sr, Zr, and Y. The depletion in Ni is also consistent with olivine fractionation, and the compatible behaviour of Cr implies the involvement of chrome spinel also. The behaviour of Ba, K, (Fig. 3f, k) and Rb (not shown) is, however, not readily explicable. The expected negative correlations with Mg are not found, and indeed Ba has a rather strong positive correlation.

Sr isotope ratios of the E–W dykes (Fig. 4, Table 2) are low (0.7037–0.7039) and they have positive ε_{Nd} (*c.* +3). The Pb isotope composition of the one E–W sample analysed (Table 2) lies close to the northern hemisphere reference line (NHRL, Hart 1984). The isotopic evidence therefore suggests that the E–W dykes are not strongly influenced by crustal contamination. Thus, it is unlikely that the apparently anomalous behaviour of the large ion lithophile elements (i.e. Ba, Rb, K) represents a crustal contamination effect. However, such behaviour remains unexplained and, in view of the restricted data set, we do not investigate this aspect of their geochemistry further, other than to highlight similar complexities in trace element geochemistry recognized by Armstrong *et al.* (1984) for the Rooi Rand dykes of the Karoo.

We conclude, largely on the basis of isotope ratios, that the E–W dykes are another example of the rare basic magmas, associated with Gondwanaland break-up, that have a dominantly asthenospheric mantle input, though we shall argue below that the source had a high Fe/Mg ratio compared with the source of mid-ocean ridge basalts (MORB).

With regard to major element geochemistry, some basaltic suites show a strong negative correlation between Si and Fe in their more primitive members, which can be interpreted in terms of experimental data (Hirose & Kushiro 1993; Kushiro 1996) as indicating variable depths of segregation (e.g. Scarrow & Cox 1995). However, there is no sign of such a correlation in the present data for the E–W suite. In fact the Fe contents, with a single exception, are remarkably uniform. Thus, if we choose to follow this model, the parental magmas of the E–W suite appear to have segregated over a very restricted depth range. However, the absolute Fe contents of liquids generated at a particular pressure are highly dependent on the Fe/Mg ratio of the source material. The parental magmas are likely to have been more primitive than the analysed samples, and we have calculated the composition of possible parental liquids by the fractional addition of olivine to the average E–W composition. The calculation is continued until the model liquids are capable of equilibration with likely mantle olivines ranging from Fo_{86} to Fo_{90} (Table 4).

In experimental melts, Fe–Si relationships are strongly dependent on the Mg No. of the starting material. In our calculated range of potential parental magmas, Fe contents are relatively high for their silica levels. Thus, comparison with the experimental melts suggests a source with a low Mg No. similar to that of the relatively Fe-rich peridotite composition HK-66 used by Hirose & Kushiro (1993), which has a Mg No. of 86, substantially more Fe-rich than most analysed mantle peridotites. This is essentially the same conclusion as that reached by Scarrow & Cox (1995) for the Skye Main Lava sequence, and by Melluso *et al.* (1995) for the Deccan picrites. Apparently, the Falkland E–W dykes were derived from a high Fe/Mg mantle source component, as were the North Atlantic and Deccan flood basalts. One intriguing possibility is that high Fe/Mg might be characteristic of the mantle plume sources which are widely invoked in the petrogenesis of large igneous provinces.

North–south dykes

Compositionally the N–S dykes are distinctive in their high SiO_2 and, mineralogically, in the presence of orthopyroxene.

Table 1. *Selected mineral analyses*

	SiO_2	TiO_2	Al_2O_3	FeO	MnO	MgO	CaO	Na_2O	K_2O	NiO	Total
North–South dykes											
Orthopyroxenes											
NEF21	52.34	0.11	2.28	10.65	0.20	28.88	1.71	0.08	0.06		96.31
NEF21	54.06	0.18	2.04	11.72	0.24	26.54	2.24	0.26	0.12		97.40
NEF21	53.68	0.11	1.02	11.99	0.26	28.44	2.13	0.05	0.04		97.72
NEF21	53.06	0.20	2.03	12.15	0.26	27.66	2.38	0.13	0.04		97.91
NEF26	52.14	0.15	2.74	10.43	0.22	28.13	2.74	0.06	0.04		96.65
NEF26	54.21	0.13	2.05	9.95	0.20	29.79	1.74	—	—		98.07
NEF26	53.45	0.15	2.21	9.88	0.16	29.85	1.98	0.05	—		97.73
NEF26	54.22	0.20	1.51	12.25	0.19	27.62	2.27	0.06	—		98.32
NKF33	54.99	0.15	1.09	12.71	0.26	27.88	2.30	0.10	—		99.48
NKF33	54.01	0.22	1.17	16.50	0.27	25.13	2.26	—	—		99.56
NKF33	54.52	0.22	1.19	14.08	0.34	26.84	2.28	0.08	—		99.55
NKF33	54.52	0.18	2.65	10.22	0.18	29.88	1.85	—	—		99.56
NKF39	52.14	0.24	4.34	13.95	0.23	23.34	2.97	0.10	—		97.21
Mg-pigeonite											
NEF21	58.56	0.27	4.10	13.02	0.22	20.28	3.99	0.09	0.17		100.71
NEF26	51.67	0.31	1.01	19.81	0.43	20.89	4.75	0.03	—		98.96
NPF50	54.14	0.15	1.10	14.72	0.32	24.11	4.67	0.45	0.05		99.29
NPF50	52.76	0.11	4.02	13.48	0.35	22.18	4.86	0.08	0.08		98.29
NPF50	53.56	0.15	2.05	14.32	0.34	22.96	4.97	0.25	0.05		98.65
NKF33	53.14	0.27	0.86	18.79	0.44	21.26	4.39	0.37	0.08		99.60
NKF33	51.53	0.34	0.91	20.15	0.40	20.67	4.95	0.11	—		99.06
Augite											
NEF21	51.51	0.77	2.09	11.83	0.27	18.66	12.95	0.03	0.09		98.20
NEF21	50.34	0.48	2.34	11.28	0.23	16.02	15.97	0.22	0.05		96.93
NPF50	52.48	0.37	1.63	13.66	0.33	15.96	15.02	0.19	0.03		99.67
NPF50	50.95	0.26	1.97	8.00	0.26	16.64	17.68	0.23	0.06		96.05
NPF50	50.86	0.33	1.76	11.68	0.29	18.36	13.12	0.12	0.06		96.58
NEF26	52.71	0.45	2.72	8.59	0.22	17.61	17.31	0.29	0.04		99.94
NEF26	51.40	0.50	2.51	8.96	0.23	16.73	18.15	0.16	—		98.64
NKF33	52.65	0.43	1.84	9.31	0.25	16.58	17.95	0.23	—		99.24
NKF33	53.02	0.30	1.59	9.73	0.23	17.32	16.64	0.20	0.04		99.07
NKF33	50.66	0.46	1.58	13.37	0.28	15.48	14.96	0.34	0.05		97.18
NKF33	52.61	0.34	1.80	9.36	0.25	18.11	16.10	0.28	0.04		98.89
NKF39	50.49	0.66	1.90	13.85	0.28	14.25	16.78	0.07	0.05		98.33
NKF39	52.24	0.45	1.95	9.33	0.19	16.14	18.50	0.21	0.03		99.04
NKF39	53.38	0.22	1.42	10.29	0.31	19.80	12.91	0.13	0.07		98.53
Plagioclase											
NEF26	52.72		28.14				11.99	4.55	0.26		97.66
NEF26	50.62		29.51				13.48	3.77	0.18		97.56
NEF26	52.04		27.98				12.54	4.18	0.21		96.95
NEF26	51.20		28.93				13.75	3.83	0.21		97.92
NEF26	51.54		27.35				12.19	3.99	0.24		95.31
NKF33	54.15		25.87				9.80	4.63	0.50		94.95
NKF33	52.37		28.67				12.59	4.03	0.23		97.89
NKF33	52.20		28.35				12.04	4.47	0.24		97.30
NKF33	54.73		25.34				10.42	5.64	0.27		96.40
NKF33	53.19		28.18				11.96	4.40	0.28		98.01
NKF33	52.40		27.82				11.50	4.43	0.31		96.46
NKF39	57.15		24.76				9.68	4.67	0.42		96.68
NKF39	53.60		27.62				11.29	4.65	0.33		97.49
NKF39	51.07		28.03				13.21	3.86	0.19		96.36
East–West dykes											
Olivine											
ECF11	37.65		—	14.87	0.26	44.82	0.27	—	—	0.23	98.10
ECF11	39.10		—	15.63	0.27	43.96	0.40	—	—	0.20	99.56
ECF11	39.86		—	14.85	0.22	45.97	0.27	—	—	0.26	101.43
ECF12	40.09		—	14.63	0.23	45.22	0.27	—	—	0.26	100.70
ECF49	40.05		—	16.30	0.22	42.64	0.34	—	—	0.17	99.72
ECF49	39.25		—	15.76	0.24	42.34	0.30	—	—	0.18	98.07
ECF49	40.54		—	15.18	0.27	45.06	0.27	—	—	0.23	101.55
Plagioclase											
ECF11	50.52		29.83	0.65	—	—	14.14	3.21	0.11	—	98.46
ECF11	52.46		29.20	0.65	—	—	13.30	3.76	0.14	—	99.51
ECF11	51.34		29.02	0.91	—	—	12.55	4.11	0.17	—	98.10
ECF12	49.51		29.10	0.61	—	—	13.26	3.61	0.13	—	96.22
ECF12	49.83		30.01	0.52	—	—	13.84	3.58	0.15	—	97.93
ECF49	51.75		28.96	1.10	—	—	13.53	3.45	0.15	—	98.94
ECF49	50.30		30.46	0.54	—	—	13.99	3.50	0.11	—	98.90

Table 2. *Whole rock analyses*

	North–South dykes														
Sample	NAF1	NBF2	NBF3	NDF8	NEF9	NEF10	NGF15	NGF16	NHF17	NEF20	NEF21	NEF22	NEF23	NEF24	NEF25
SiO_2	53.32	54.12	54.24	53.16	53.18	53.13	53.68	53.18	54.07	53.32	53.24	53.48	53.31	53.32	53.32
TiO_2	0.98	1.00	1.08	0.95	0.90	0.93	1.31	0.92	1.32	1.01	0.97	0.97	0.98	0.99	0.97
Al_2O_3	13.98	15.20	14.90	13.23	13.48	14.07	13.38	12.98	13.30	14.51	14.04	13.90	14.33	14.22	14.26
Cr_2O_3	0.06	0.04	0.03	0.09	0.09	0.07	0.01	0.10	0.01	0.05	0.07	0.07	0.06	0.06	0.06
Fe_2O_3(t)	11.41	10.91	11.52	11.87	11.31	11.22	13.37	11.57	13.91	11.14	11.31	11.65	11.31	11.49	11.38
MnO	0.17	0.16	0.16	0.18	0.18	0.20	0.24	0.20	0.22	0.21	0.22	0.18	0.17	0.18	0.17
MgO	7.86	6.30	5.74	9.30	9.27	8.39	4.87	9.51	4.80	7.21	7.97	8.30	7.57	7.74	8.00
CaO	8.84	9.20	9.23	8.81	8.59	8.46	8.58	8.67	8.70	8.84	9.07	9.11	8.99	9.16	9.11
Na_2O	2.18	2.71	2.48	2.10	2.19	2.35	2.48	1.93	2.52	2.44	2.14	2.21	2.35	2.33	2.30
K_2O	0.77	0.69	0.88	0.63	0.75	0.92	1.23	0.47	1.18	0.87	0.65	0.64	0.77	0.70	0.74
P_2O_5	0.14	0.14	0.16	0.13	0.12	0.13	0.18	0.12	0.19	0.14	0.13	0.13	0.13	0.13	0.13
Total	99.71	100.47	100.42	100.45	100.06	99.87	99.33	99.65	100.22	99.74	99.81	100.64	99.97	100.32	100.44
Rb	22	18	26	17	22	28	30	13	34	26	18	18	22	20	21
Sr	218	300	273	197	256	322	189	199	178	258	201	199	243	222	253
Y	24	25	27	24	25	25	46	27	39	25	23	23	24	24	24
Zr	111	110	118	100	97	100	215	94	214	106	104	101	102	104	102
Nb	6	7	7	6	6	5	17	6	16	6	6	6	6	7	6
Pb	8	7	8	7	6	12	9	5	6	7	7	8	8	8	8
Zn	87	97	89	85	79	83	117	81	109	82	82	87	78	83	83
Cu	75	66	72	56	79	86	166	102	166	79	77	92	84	79	80
Ni	113	74	67	128	133	113	47	164	39	98	101	123	98	98	101
Co	50	40	41	52	52	45	55	57	42	45	46	50	44	47	44
Cr	397	235	198	540	589	479	22	648	21	371	442	474	402	403	418
V	218	212	221	227	218	226	294	230	298	244	233	235	230	236	225
Ba	392	376	494	563	1235	2229	494	366	371	2020	413	499	1257	738	1324
Sm	3.69	3.70			3.09			3.41	5.05					3.43	
Nd	15.03	15.68			12.21			12.80	24.93					13.45	
$^{87}Sr/^{86}Sr_{(0)}$	0.71031	0.71202	0.71195	0.70937	0.71147			0.70912	0.70737			0.70893	0.71040	0.70980	0.71071
± 2 SE	± 4	± 5	± 4	± 4	± 4			± 4	± 3			± 4	± 4	± 4	± 7
$^{87}Sr/^{86}Sr_{(i)}$	0.70931	0.71135	0.71101	0.70847	0.71060			0.70877	0.70586			0.70835	0.70985	0.70887	0.71019
$^{143}Nd/^{144}Nd_{(0)}$	0.512154	0.512014			0.512293			0.512314	0.512429					0.512321	
± 2 SE	± 8	± 6			± 5			± 6	± 6					± 6	
$^{143}Nd/^{144}Nd_{(i)}$	0.511969	0.511837			0.512103			0.512114	0.512277					0.512130	
ε_{Nd}	− 8.3	− 10.9			− 5.7			− 5.5	− 2.3					− 5.1	
$^{206}Pb/^{204}Pb_{(0)}$					17.860				18.306			17.867	17.794	17.776	17.851
± 2 SE					± 13				± 33			± 8	± 1	± 13	± 6
$^{207}Pb/^{204}Pb_{(0)}$					15.612				15.564			15.656	15.611	15.575	15.601
± 2 SE					± 10				± 22			± 8	± 13	± 14	± 6
$^{208}Pb/^{204}Pb_{(0)}$					37.973				38.565			38.100	38.011	37.893	37.937
± 2 SE					± 29				± 63			± 24	± 21	± 31	± 15

Table 2. *Continued*

Sample	North–South dykes														
	NEF26	NKF27	NKF28	NKF29	NKF30	NKF31	NKF32	NKF33	NKF34	NLF35	NLF36	NKF37	NKF38	NKF39	NMF40
SiO_2	53.38	53.58	53.43	53.46	53.75	53.47	53.29	53.50	52.96	53.36	53.47	53.78	54.24	53.85	54.22
TiO_2	0.98	0.98	0.95	1.01	0.98	0.96	0.94	1.00	0.92	1.04	1.02	1.02	1.04	0.97	1.03
Al_2O_3	14.01	14.21	14.56	14.10	14.94	14.45	14.62	14.82	13.31	14.74	14.89	14.76	15.17	14.35	15.26
Cr_2O_3	0.07	0.07	0.06	0.06	0.05	0.06	0.06	0.05	0.09	0.04	0.04	0.05	0.03	0.06	0.03
Fe_2O_3(t)	11.59	11.44	11.20	11.67	11.21	11.27	11.15	11.17	11.43	11.21	10.96	11.56	11.10	11.34	11.08
MnO	0.20	0.17	0.17	0.17	0.16	0.17	0.16	0.17	0.17	0.19	0.17	0.17	0.16	0.17	0.16
MgO	8.24	7.86	7.43	7.64	7.25	7.63	7.39	7.03	8.87	6.15	6.30	7.03	6.02	7.65	6.13
CaO	8.92	9.14	9.01	8.92	9.14	9.05	9.20	8.90	8.43	8.45	8.33	9.08	9.31	9.04	9.46
Na_2O	2.25	2.21	2.37	2.31	2.49	2.31	2.32	2.42	2.18	2.45	2.46	2.55	2.57	2.41	2.54
K_2O	0.64	0.72	0.76	0.81	0.86	0.83	0.82	1.02	0.61	1.27	1.38	0.87	0.97	0.77	0.89
P_2O_5	0.13	0.14	0.14	0.14	0.13	0.13	0.13	0.14	0.13	0.14	0.14	0.14	0.14	0.13	0.14
Total	100.41	100.52	100.08	100.29	100.96	100.33	100.08	100.22	99.10	99.04	99.16	101.01	100.75	100.74	100.94
Rb	18	22	23	26	26	24	25	34	18	39	42	26	28	23	27
Sr	196	245	264	269	301	280	289	447	187	500	685	318	341	294	273
Y	24	25	23	24	25	22	22	24	28	25	24	23	25	25	24
Zr	101	106	105	110	107	105	103	109	97	115	112	110	116	107	108
Nb	5	6	7	6	6	5	6	5	5	6	6	6	7	6	7
Pb	9	9	8	7	8	7	7	7	7	6	6	8	10	8	9
Zn	82	86	82	87	86	85	85	85	93	85	84	87	90	88	91
Cu	81	67	68	74	71	66	69	67	101	85	87	71	82	68	72
Ni	110	108	99	104	99	101	96	89	237	84	84	88	76	108	69
Co	47	48	44	45	46	43	41	43	65	48	43	45	44	49	44
Cr	469	421	361	388	346	396	366	320	611	243	233	313	198	401	212
V	228	215	213	221	217	219	217	220	230	248	239	228	226	223	222
Ba	473	441	346	679	787	765	794	805	394	4679	5103	501	734	436	915
Sm				3.62			3.35						3.88		3.65
Nd				14.56			13.40						15.52		14.91
$^{87}Sr/^{86}Sr_{(0)}$		0.71095		0.71202	0.71250	0.71236	0.71202						0.71317	0.71229	0.71186
± 2 SE		± 4		± 3	± 3	± 5	± 6						± 5	± 6	± 5
$^{87}Sr/^{86}Sr_{(i)}$		0.71026		0.71107	0.71162	0.71149	0.71152						0.71232	0.71188	0.71088
$^{143}Nd/^{144}Nd_{(0)}$				0.512178			0.512189						0.512176		0.512056
± 2 SE				± 7			± 6						± 6		± 6
$^{143}Nd/^{144}Nd_{(i)}$				0.511992			0.512001						0.511988		0.511872
ε_{Nd} ^{190}				− 7.8			− 7.7						− 7.9		− 10.2
$^{206}Pb/^{204}Pb_{(0)}$		17.982		17.958	17.867	17.949							18.031	17.980	18.201
± 2 SE		± 6		± 11	± 8	± 5							± 13	± 4	± 14
$^{207}Pb/^{204}Pb_{(0)}$		15.620		15.621	15.656	15.629							15.606	15.623	15.647
± 2 SE		± 7		± 9	± 11	± 5							± 11	± 4	± 11
$^{208}Pb/^{204}Pb_{(0)}$		38.135		38.166	38.100	38.155							38.090	38.142	38.270
± 2 SE		± 14		± 21	± 28	± 11							± 3	± 13	± 30

Table 2. *Continued*

	East–West dykes											Mount Alice		
Sample	NMF41	ECF7	ECF11	ECF12	ECF13	ECF14	ENF42	ECF43	ECF44	ECF48	ECF49	MA1	MA2	MA3
SiO_2	54.32	50.17	49.03	49.01	48.75	49.20	49.90	50.48	50.71	50.18	49.41	47.75	48.47	47.60
TiO_2	1.03	1.19	1.07	1.04	1.13	1.03	1.21	1.32	1.33	1.09	1.14	1.40	1.53	1.51
Al_2O_3	15.07	14.96	14.23	14.12	14.09	14.20	14.49	15.11	15.31	15.73	13.83	16.53	16.55	16.19
Cr_2O_3	0.04	0.09	0.12	0.13	0.11	0.13	0.08	0.06	0.05	0.08	0.13	0.02	0.02	0.02
Fe_2O_3(t)	11.40	11.89	11.65	11.49	11.73	11.67	12.01	11.98	11.92	10.92	12.06	12.97	12.99	13.21
MnO	0.17	0.18	0.18	0.17	0.17	0.17	0.18	0.18	0.17	0.16	0.18	0.20	0.19	0.19
MgO	6.38	7.97	10.49	11.40	9.70	11.24	9.16	7.58	7.42	8.37	11.02	8.31	8.22	7.97
CaO	9.37	10.46	10.04	9.84	10.05	10.10	10.22	10.79	10.94	10.72	9.77	10.10	9.49	10.37
Na_2O	2.55	2.58	2.34	2.26	2.43	2.26	2.58	2.54	2.59	2.64	2.33	2.66	2.78	2.59
K_2O	0.93	0.36	0.33	0.32	0.35	0.31	0.37	0.30	0.26	0.34	0.36	0.38	0.40	0.33
P_2O_5	0.14	0.12	0.11	0.10	0.11	0.11	0.12	0.13	0.11	0.12	0.16	0.20	0.17	
Total	101.40	99.97	99.59	99.88	98.62	100.42	100.32	100.47	100.70	100.34	100.35	100.48	100.84	100.15
Rb	28	9	9	10	9	8	9	9	8	9	10	10	9	8
Sr	307	296	268	308	269	307	282	284	283	307	262	396	787	291
Y	23	20	17	15	17	15	19	23	24	16	17	19	18	20
Zr	106	81	75	72	80	72	85	89	91	73	82	90	89	93
Nb	6	6	6	5	6	6	5	6	6	5	6	7	7	7
Pb	8	5	5	4	4	6	5	8	5	6	6	5	4	4
Zn	86	77	82	76	85	79	77	95	93	71	84	76	87	84
Cu	67	83	95	92	91	90	82	81	83	84	92	92	54	98
Ni	75	177	275	263	236	263	174	127	113	152	316	116	103	114
Co	38	53	57	58	58	62	54	47	45	50	66	58	54	59
Cr	223	489	792	708	707	724	449	343	310	470	892	89	86	101
V	219	225	223	210	234	207	237	266	265	216	220	240	209	254
Ba	365	145	163	218	167	210	144	126	118	171	152	827	1719	808
Sm	3.51				2.70		2.76		3.33			3.34		
Nd	14.42				9.90		10.43		11.95			8.88		
$^{87}Sr/^{86}Sr_{(0)}$	0.71231				0.70401		0.70379		0.70382			0.70516		
± 2 SE	± 6				± 5		± 4		± 4			± 5		
$^{87}Sr/^{86}Sr_{(i)}$	0.71173				0.70390		0.70369		0.70373			0.70495		
$^{143}Nd/^{144}Nd_{(0)}$	0.512032				0.512762		0.512752		0.512768			0.512816		
± 2 SE	± 6				± 5		± 6		± 6			± 6		
$^{143}Nd/^{144}Nd_{(i)}$	0.511849				0.512558		0.512553		0.512559			0.512534		
ε_{Nd} [190]	− 10.6				3.2		3.1		3.2			2.8		
$^{206}Pb/^{204}Pb_{(0)}$	18.222				18.214							17.910		
± 2 SE	± 8				± 17							± 15		
$^{207}Pb/^{204}Pb_{(0)}$	15.696				15.471							15.500		
± 2 SE	± 7				± 18							± 13		
$^{208}Pb/^{204}Pb_{(0)}$	38.508				37.581							37.573		
± 2 SE	± 18				± 45							± 31		

Table 3. *End-members and extract calculation for the E–W dykes*

	Basic	Evolved	Enrichment factor	Correlation with MgO	Olivine
SiO_2	49.06	50.31		−0.87	38.91
TiO_2	1.01	1.34	1.33	−0.82	—
Al_2O_3	13.91	15.69		−0.85	—
Fe_2O_3	11.89	11.71		−0.09	15.94
MgO	11.63	6.97			44.88
CaO	9.86	10.91		−0.92	0.26
Na_2O	2.23	2.64	1.18	−0.92	—
K_2O	0.30	0.30	1.00	0.27	—
P_2O_5	0.10	0.13	1.30	−0.73	—
Ba			0.53	0.79	
Rb			0.80	0.51	
Sr			1.19	−0.03	
Y			1.75	−0.82	
Zr			1.29	−0.67	
Nb			1.00	0.07	
Ni			0.32	0.94	
Co			0.65	0.90	
Cr			0.32	0.90	
V			1.30	−0.76	
	Basic	Calculated	Δ^2		
SiO_2	49.06	48.95	0.012		
TiO_2	1.01	1.18	0.029		
Al_2O_3	13.91	13.82	0.008		
Fe_2O_3	11.89	12.21	0.102		
MgO	11.63	11.48	0.023		
CaO	9.86	9.64	0.048		
Na_2O	2.23	2.33	0.010		
K_2O	0.30	0.26	0.002		
P_2O_5	0.10	0.11	0.000		
		Σ	0.234		

Estimated basic and evolved end-members and olivine composition used in mixing calculation, enrichment factors and correlation coefficients with MgO (r=0.765 for 99% significance level). The mixing calculation (after Wright & Doherty 1970) adds olivine to the evolved end-member in an attempt to simulate the basic end-member. In this calculation the proportions are: olivine 0.119, evolved end-member 0.881. Δ^2 values are squares of residuals and Σ is the sum of squares.

As shown below they also show a very distinctive fractionation behaviour.

The samples are separable into three groups (Fig. 3) on the basis of MgO content. Two samples, NHF17 and NGF15 (termed the evolved group) have MgO below 5%, and are clearly not directly related to the same fractionation trend as the more mafic samples (e.g. Fig. 3b, d, e). An intermediate group, with MgO in the range 5–7%, can then be distinguished from the remaining samples (MgO>7%—the primitive group) by generally lying slightly off the fractionation trend of the latter (e.g. Fig. 3c, d).

Fractionation of the primitive group. Fractionation was modelled by calculating first the compositions of two end-members, 'evolved' and 'primitive' (Table 5). These compositions were derived by regressing other elements against MgO (anhydrous data), and using the regression lines to estimate their concentrations at the minimum (evolved) and maximum (primitive) MgO values. Correlation coefficients with MgO, and enrichment factors for potentially incompatible elements, are also given (Table 5).

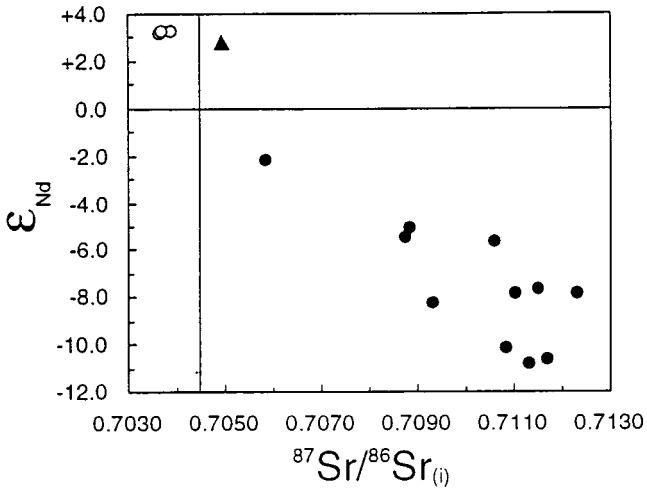

Fig. 4. Initial Nd v. Sr isotope ratios. Triangle is Mount Alice sample MA1.

Table 4. *Calculated possible parental magmas for E–W suite and their equilibrium olivine composition*

SiO_2	49.80	49.50	49.20	48.85	48.45
FeO(t)	11.14	11.20	11.23	11.21	11.18
MgO	11.40	12.50	13.70	15.10	16.80
Olivine (Fo)	86	87	88	89	90

In the silica range above, experimental equilibrium melts of three investigated dry peridotites have approximate FeO contents as follows: HK66 (Mg no.=85.3), FeO=9–11 wt%(Hirose & Kushiro 1993); PHN1611 (Mg no.=86.8), FeO=9.3–10.1 wt% (Kushiro 1996); KLB1 (Mg no.=89.6), FeO=7.8–9.1 wt% (Hirose & Kushiro 1993).

The fractionation trend of this group (Fig. 3) is at first sight similar to the olivine-dominated trend of the E–W dykes, but there are important differences. As MgO falls, Al, Ca, Si, and a range of incompatible elements (e.g. Ti, Na, K, Rb, Sr, Zr) become enriched, while Fe stays relatively constant. These are strong indications of fractionation dominated by ferromagnesian minerals. However, compared with the olivine-generated trend of the E–W dykes, the enrichment of Ca and Si are both less, as is the depletion in Ni. This points to the involvement of pyroxene, including at least some of a Ca-bearing type. Mixing calculations, bearing in mind the petrography of NKF34, were carried out based on the extraction of olivine, orthopyroxene, and clinopyroxene. The calculations are quite sensitive to mineral composition input, and it is also clear that several of the critical regression lines are based on rather poor correlations (especially MgO v. CaO and MgO v. SiO_2). There are other options also, involving extraction of pigeonite. The example given in Table 5 uses the least-evolved mineral compositions, which minimizes the amount of fractionation required—in this case 11% of solid is removed. The result is a good fit to the data, using a mixture of the calculated extract with the evolved liquid to estimate the composition of the primitive liquid. However, the calculation given is regarded as indicative only because good fits are readily obtained when the amount of fractionation is small.

The potentially incompatible elements are divided into two groups: Ti, Al, P, Zr (and possibly Na) have enrichment factors of *c.* 1.1 consistent with the result in Table 5 (the Nb factor is low, but the concentrations are near detection limit).

Table 5. *End-members and extract calculation for the primitive members of the N–S suite*

	Evolved	Primitive	Enrichment Factor	Mineral analyses in extract calculation (Fe as Fe_2O_3) Olivine	Opx	Cpx
SiO_2	53.34	53.18		39.42	54.14	52.72
TiO_2	0.99	0.91	1.08		0.15	0.26
Al_2O_3	14.74	13.10	1.13		2.24	2.46
Fe_2O_3	11.22	11.62		16.52	11.01	9.06
MgO	6.96	9.54		43.52	30.24	17.66
CaO	9.08	8.64	1.05	0.30	2.01	17.40
Na_2O	2.44	2.04	1.20			0.18
K_2O	0.87	0.57	1.53			0.04
P_2O_5	0.13	0.12	1.11			
Rb	27	15	1.75			
Zr	109	95	1.14			
Sr	23	26	0.91			
Y	306	181	1.69			
Nb	6.0	5.7	1.04			
Extract calculation						
	Primitive	Estimated primitive	Δ^2	Extract		
SiO_2	53.18	53.01	0.029			
TiO_2	0.91	0.90	0.000	Olivine	0.026	
Al_2O_3	13.10	13.31	0.044	Cpx	0.021	
Fe_2O_3	11.62	11.30	0.101	Opx	0.063	
MgO	9.54	9.60	0.004			
CaO	8.64	8.58	0.004	Liquid	0.891	
Na_2O	2.04	2.18	0.019			
K_2O	0.57	0.78	0.042			
			$\Sigma=0.244$			

On the other hand, K, Rb and Sr have enrichment factors substantially higher (*c.* 1.5–1.8). As we show below, crustal contamination is highly evident in the suite, and we regard the second group as strongly influenced by this process. Conversely, we assume that the first group may be used, like the major elements in the mixing calculation, to interpret fractional crystallization history as a first approximation. The assumption is that concentrations of these elements in original magmas and supposed contaminants were not so enormously different that relatively small amounts of contamination can seriously distort the calculations.

Accepting $F=0.89$ in Rayleigh fractionation calculations, we next determine the apparent bulk distribution coefficients (D) of the potentially compatible elements Cr and Ni, which work out respectively at 7.6 and 5.2; note that $D_{Cr}>D_{Ni}$. Y also appears to be fairly compatible. Similar calculations produce an apparent D_Y of 1.9, but, given the uncertainty in the regression line used to calculate end-member compositions, probably it is safer to regard this result as *c.* 1.

Published distribution coefficients for these elements in these phases are highly diverse (especially with regard to basaltic liquids versus andesitic liquids, and given the high SiO_2, but also high MgO, that choice would be problematic). However, all agree (see Rollinson 1993, for compilations) that $D_{Cr}>D_{Ni}$ in pyroxenes, the reverse being the case in olivine. Also, for the phases concerned, high D_Y is only appropriate for pyroxenes. The trace element data thus support a dominant role for pyroxene fractionation in the evolution of this suite. The behaviour of SiO_2 and Al_2O_3 v MgO (Fig. 3a, d) is entirely consistent with this. The first demands a high-SiO_2 extract, too rich in SiO_2 for olivine alone, the second a low-MgO extract, too poor in MgO for olivine alone.

However, in view of a subsequent section discussing the relationships between radiogenic isotopes and variation in elemental abundances, which strongly imply fractional crystallization accompanied by assimilation of crustal rocks or melts, the results of these closed system crystal fractionation calculations should be regarded as only a first approximation. The variations in the enrichment factors for potentially incompatible elements also need to be addressed.

The evolved members of the N–S suite. We noted above two evolved examples of N–S dykes, which, if they are related to the rest of the suite at all, have clearly undergone advanced degrees of gabbro fractionation (see Fig. 3—note strong enrichment in Fe and Ti, and depletion in Al and Sr). However, one of these samples has initial $^{87}Sr/^{86}Sr$ *c.* 0.705 (see Table 2). This is a typical value for the Mafika Lisiu magma type (Marsh *et al.* 1997) of the Lesotho Formation of the Karoo (see Table 6), and it is possible that they are evolved representatives of this suite. The Lively Island dyke, which is also a close analogue of the Mafika Lisiu magma-type, also has a N–S trend. In any event, the large compositional differences between these evolved samples and the next most basic members of the N–S suite (the intermediate group), do not allow us to conclude safely that they are directly related.

The intermediate group of the N–S suite. Figure 3 shows the scattered nature of these compositions, details of which are difficult to interpret. Some of the elemental relationships with

Table 6. *Comparison of average analyses of Gondwanaland dykes*

	1 N–S dykes	2 Hangnest dolerites	3 Kaai River	4 Kirkpatrick basalts	5 Lively Island	6 Mafika Lisiu	7 E–W dykes	8 Primitive Rooi Rand
SiO_2	53.53	53.92	54.17	54.15	51.87	51.50	49.75	49.80
TiO_2	0.98	1.10	0.87	0.62	0.80	0.95	1.19	1.62
Al_2O_3	14.36	15.80	15.23	15.20	16.15	15.69	14.53	14.75
Fe_2O_3(t)	11.34	9.99	10.07	10.13	11.20	10.96	11.94	13.00
MnO	0.18	0.16	0.20	0.18	0.18	0.16	0.18	—
MgO	7.52	6.49	6.58	7.03	6.09	7.01	9.26	7.37
CaO	8.96	9.23	10.05	10.89	10.42	10.69	10.15	12.02
Na_2O	2.35	2.20	2.12	1.77	2.39	2.17	2.44	2.22
K_2O	0.81	0.89	0.56	0.60	0.70	0.70	0.35	0.30
P_2O_5	0.13	0.22	0.15	0.09	0.16	0.16	0.12	0.10
Rb	24	22	21	24	17	12	10	5.4
Sr	287	201	214	192	220	192	282	167
Y	24	27	28	26	22	24	19	24
Zr	106	156	118	95	92	94	83	72
Nb	6	5	4.8	5	11	4.9	6	3.6
Pb	8	—	6	—	5.7	2.9	6	—
Zn	85	91	83	—	89	86	83	80
Cu	77	19	63	—	62	87	88	160
Ni	105	4	51	—	64	94	195	80
Co	46	40	38	—	41	48	54	55
Cr	383	368	264	—	169	283	553	200
V	225	193	240	—	181	240	235	275
Ba	1039	318	173	192	205	177	191	50
	$n=30$	$n=10$	$n=24$	$n=17$	$n=2$	$n=59$	$n=12$	
$^{87}Sr/^{86}Sr(i)$	0.7105	0.7086	0.7077	0.7115	0.7056	0.7054	0.7038	0.7040

1. Average N–S dykes, West Falkland excluding the two most evolved samples. 2. Average Hangnest dolerite (Duncan *et al.* 1984). 3. Average Kraai River basalt (Duncan *et al.* 1984). 4. Average Kirkpatrick basalt (Siders & Elliot 1985). 5. Average Lively Island dolerite. 6. Average Mafika Lisiu Unit basalt, Lesotho Formation (Duncan *et al.* 1984). 7. Average E–W dykes, West Falkland. 7. Estimate of most primitive type from Rooi Rand dolerites of Armstrong *et al.* (1984).

MgO are similar to the expected continuation of the primitive samples trend (e.g. Fe, Fig. 3b). Others are slightly off the main trend (e.g. Na, Al, Fig. 3c, d), and a few samples are far off-trend (e.g. Ca, Sr, Fig. 3e, l). Probably some plagioclase has been introduced into the fractionating assemblage. Samples from this group do, however, contribute to the correlations between elemental concentrations and initial $^{87}Sr/^{86}Sr$ shown in Fig. 5.

Isotope geochemistry of the N–S suite. The N–S dykes all have elevated initial (190 Ma) $^{87}Sr/^{86}Sr$ (0.7059–0.7123) and low initial $^{143}Nd/^{144}Nd$ ($\varepsilon_{Nd} = -2.3$ to -10.9). However, the lowest initial $^{87}Sr/^{86}Sr$ and highest ε_{Nd} is found in a sample from the evolved group of dykes and, as noted above, there is no strong evidence to link these samples to the bulk of the N–S suite. Thus we find no compelling evidence for N–S suite samples with initial $^{87}Sr/^{86}Sr < 0.708$ and $\varepsilon_{Nd} > -5$. Such compositions extend beyond the range observed in MORB and ocean island basalts (OIB) and therefore demand the involvement of a component whose influence does not dominate the isotopic compositions of basalts erupted in intraoceanic settings. Given the continental association it has become commonplace to locate such a component in the continental (crust or mantle) lithosphere.

In addition to their 'enriched' isotopic compositions, the N–S suite displays correlations between isotope ratios (illustrated here by initial $^{87}Sr/^{86}Sr$) and elemental abundances (Fig. 5) that can themselves be related to the degree of crystal fractionation. Correlations significant at the 99% level exist between initial $^{87}Sr/^{86}Sr$ and Si, Al, Na, K, Rb and Sr (all positive) and Fe, Mg, Ni, Co and Cr (all negative). It is possible that such correlations could be generated by simple physical mixing between basic and acid magmas but this is not demanded by the data. Rather, we prefer to interpret these coherent trends as representing combined assimilation of country rocks coupled with fractional crystallization (AFC).

The origin of high $^{87}Sr/^{86}Sr$ and low $^{143}Nd/^{144}Nd$ basalts has been an issue of great controversy for many years with cogent arguments being advanced in support of both contamination within the continental crust (e.g. Menzies *et al.* 1984; Cox & Hawkesworth 1984) and 'mobilization' of sub-crustal enriched mantle material (e.g. Carlson 1984; Hawkesworth *et al.* 1984). In the case of the Falklands N–S suite, the argument that most of the isotopic variation within the N–S suite can be attributed to contamination seems compelling because it is intimately associated with changes in differentiation indices. The differentiation indices we choose to illustrate this point are themselves strongly correlated with Mg No. (not shown) and the latter is expected to remain buffered so long as the magma remains in equilibrium with mantle olivine. The observed correlations are therefore most likely to originate through processes after separation from the mantle source. The strong correlations with elemental data imply a contaminant with high $^{87}Sr/^{86}Sr$ (>0.712), and the large enrichment factors for

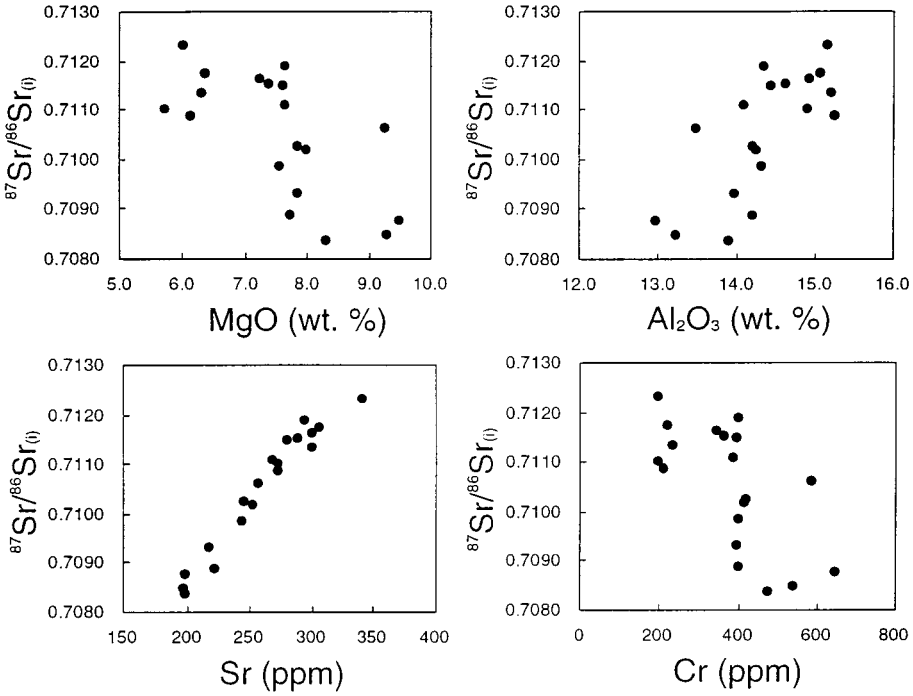

Fig. 5. N–S suite: variations in initial (190 Ma) $^{87}Sr/^{86}Sr$ with selected elemental abundances.

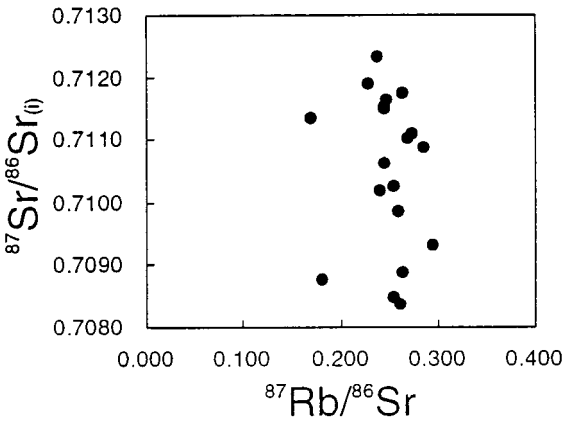

Fig. 6. N–S suite: initial $^{87}Sr/^{86}Sr$ v. $^{87}Rb/^{86}Sr$.

K, Rb and Sr suggest the contaminant to have been rich in those elements relative to the uncontaminated magmas.

Despite the evidence of crustal contamination we have no N–S samples (except the potentially unrelated evolved group) with initial $^{87}Sr/^{86}Sr$ below about 0.708. This is still an elevated composition compared with most mantle-derived rocks and it may well be the case that the crustal contamination we have described was itself responsible for only the isotope variation recognized and was superimposed upon already elevated $^{87}Sr/^{86}Sr$ in parental magmas which originated from mantle with higher than usual $^{87}Sr/^{86}Sr$. Indeed, despite strong correlations between $^{87}Sr/^{86}Sr$ and Rb and Sr concentrations, there is no comparable correlation between $^{87}Sr/^{86}Sr$ and $^{87}Rb/^{86}Sr$ (Fig. 6). The Rb/Sr ratios of all the N–S dykes are high and the crustal contamination process does not increase Rb/Sr. There is therefore no evidence to support extrapolation to a low Rb/Sr parental composition, and we conclude, as did Hergt *et al.* (1989) for the Tasmanian Jurassic dykes, that a mantle source with elevated Rb/Sr and consequently high $^{87}Sr/^{86}Sr$ cannot be ruled out.

Pb isotope data offer further insights into the likely mantle source of the N–S dykes. Firstly, the Pb isotope data (Fig. 7) also record the AFC process, being well correlated with MgO and initial $^{87}Sr/^{86}Sr$ (note that Pb isotope data are not age-corrected due to lack of U concentrations and the likelihood that measured U would anyway be affected by relatively recent alteration). Thus, the proposed contamination process seems to have generated the observed range in Pb isotope compositions. That contamination process led to an increase in $^{206}Pb/^{204}Pb$ so that the least radiogenic Pb isotope compositions are likely to be most representative of the parental mantle-derived composition. Even if the least evolved N–S samples were themselves crustally contaminated to some degree, identification of the uncontaminated end-member would require extrapolation towards low $^{206}Pb/^{204}Pb$ into a portion of the Pb–Pb isotope diagrams (Fig. 8) that is very rarely occupied by basaltic rocks. Indeed, a measure of the rarity of such Pb isotope compositions is that the least contaminated N–S dykes plot close to the 4.55 Ga single-stage geochron (Fig. 8). The very failure of most mantle and crustal rocks to lie on the geochron is at the heart of the famous 'Pb paradox'.

Thus, the N–S dykes which most closely approach the parental composition prior to AFC still have Sr, Nd and Pb isotope ratios that fall outside the ranges observed in oceanic basalts. Critically, simply extending the $^{206}Pb/^{204}Pb$–$^{87}Sr/^{86}Sr$ (Fig. 7) contamination trend back to $^{87}Sr/^{86}Sr$ values more typical of asthenosphere-derived basalts does not result in a Pb isotope composition found in any MORB or OIB. Thus the evidence is strengthened that even the uncontaminated N–S end-member requires an exotic, and by implication lithospheric mantle, component.

More detailed interpretation of the Sr–Nd–Pb isotope variations is beyond the scope of this paper and the present data base. However, we note that the N–S dykes have Pb isotope characteristics which are quite different from other

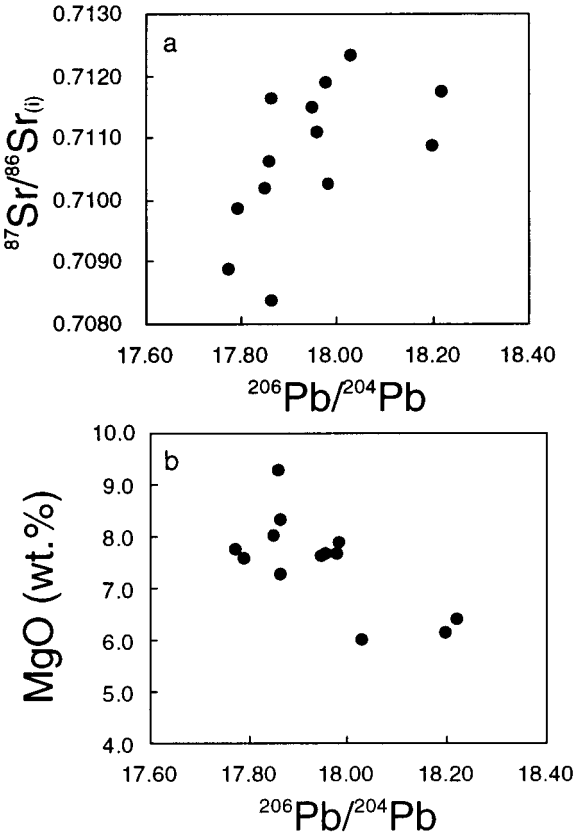

Fig. 7. N–S suite: $^{206}Pb/^{204}Pb$ v. (**a**) $^{87}Sr/^{86}Sr$ and (**b**) MgO to illustrate shift to more radiogenic Pb associated with increasing $^{87}Sr/^{86}Sr$ and decreasing MgO through assimilation fractional crystallization.

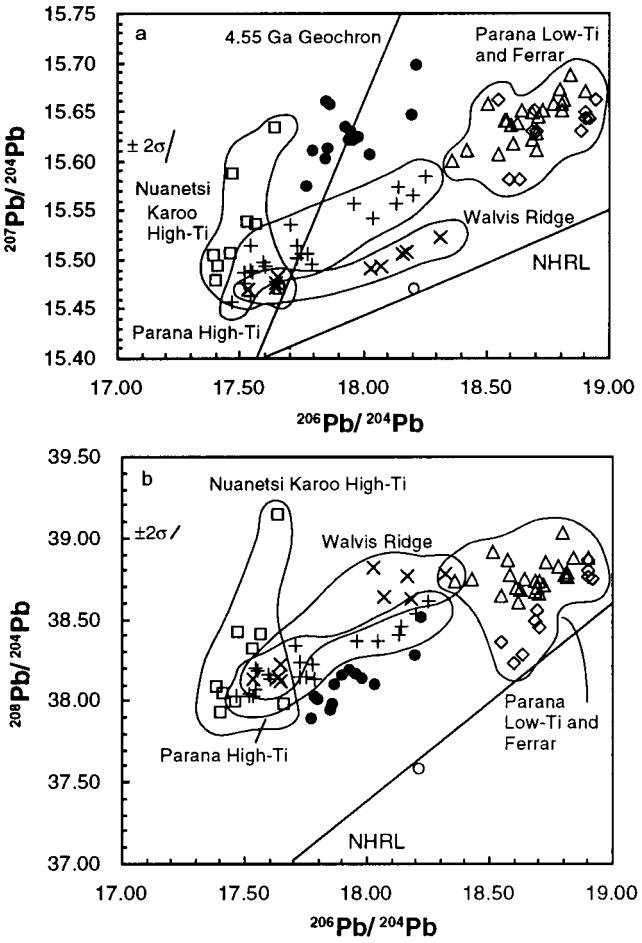

Fig. 8. (**a**) $^{207}Pb/^{204}Pb$ v. $^{206}Pb/^{204}Pb$ and (**b**) $^{208}Pb/^{204}Pb$ v. $^{206}Pb/^{204}Pb$ for N–S dykes (solid circles) and one E–W dyke (open circle) compared with various Mesozoic Gondwanan CFB (Ellam & Cox 1991; Peate 1991; Hergt *et al.* 1989; Molzahn *et al.* 1996) and Walvis ridge basalts (Richardson *et al.* 1982) which are thought to include a contribution from Gondwanan lithospheric mantle (Hawkesworth *et al.* 1986). NHRL is northern hemisphere reference line (Hart 1984). Parana Low-Ti basalts are represented by open triangles, Ferrar dolerites by open diamonds. All data are present day but Ferrar data were obtained on feldspars and therefore approach initial ratios (Molzahn *et al.* 1996).

Gondwanaland low-Ti basalts (e.g. Hergt *et al.* 1989, 1991; Peate 1991; Peate & Hawkesworth 1996) but which show some affinity with high-Ti Gondwanan basalts elsewhere (Ellam & Cox 1991). Moreover, low-Ti basalts from the Karoo (Marsh *et al.* 1992, 1993) share the unusual N–S Pb isotope signature.

Comparison with other Gondwanaland basalts

The very wide-spread vulcanism which accompanied the break-up of Gondwanaland is divided into a number of provinces on the basis of the different, mainly basic, magma types present. In Table 6 average analyses for the Falklands dolerite suites are compared with averages from other places, in order to study further magmatic provinciality.

The N–S dolerites are of a high-silica, low-Ti, type which is relatively rare in the Karoo in Africa, with the closest compositional analogues being the Kraai River magma type in the northeast Cape and dolerites from the Hangnest sill near Calvinia in the western Karoo which constitute the Hangnest magma type (Marsh & Eales 1984). However, closely comparable rocks are widespread in Coats Land, the Transantarctic Mountains and Tasmania; e.g., Series 1 Coats Land dolerites (Brewer *et al.* 1992), Ferrar basalts and dolerites (Molzahn *et al.* 1996), Kirkpatrick Basalts (Siders & Elliot, 1985), Tasmanian Dolerites (Hergt *et al.* 1989). Note that all these types have high initial $^{87}Sr/^{86}Sr$ ratios (see Table 6).

Although the Lively Island dyke has a north–south trend it is geochemically quite different from the West Falkland N–S suite, and is separated geographically. The dyke is extremely closely comparable to the average composition of the wide-spread Mafika Lisiu unit (Marsh *et al.* 1997) of the Lesotho Formation (Duncan *et al.* 1984) in the Karoo (Table 6), sharing the slightly high Si, low Ti, and distinctive high Al, as well as the slightly high initial Sr isotope ratio (0.705–0.706). This is also not surprising in view of the pre-drift position of the islands.

The E–W dolerites are quite distinct from the types above. Although they are also low-Ti types, they are less Si-rich and show low initial $^{87}Sr/^{86}Sr$ values (0.7037–0.7039). Such compositions, like those of the N–S dolerites, are also uncommon in the Karoo. In fact, broadly comparable rocks are only represented by the Rooi Rand dolerites of the southern Lebombo (see Table 6) and by the Horingbaai dolerites of Etendeka (Duncan *et al.* 1990). These latter suites are the only ones in the Karoo–Etendeka province to have such low initial

Sr isotope ratios (Bristow *et al.* 1984). However, it is notable that though the possible correlative dykes from the Falkland Islands in their pre-drift position do lie on the southerly extension of the N–S Rooi Rand dyke swarm, they were nevertheless emplaced with an approximately E–W strike.

The Mount Alice dykes, represented by three analyses (Table 2), are silica-poor by comparison with almost all known Gondwanaland basaltic/doleritic rocks except some of the picrite basalts from the North Lebombo and Nuanetsi (now Mwenezi) in the Karoo Province (Bristow 1984). However, the Nuanetsi–N Lebombo rocks are of high-Ti affinity and evolved members of the picrite basalt suite, which have silica and magnesium contents approaching those of the Mount Alice dykes, are very poor in alumina by comparison. The only near-match we can find for the Mount Alice dykes is represented by the most Mg-rich lavas of the Sabie River Basalt Formation (SRBF) (Cox & Bristow 1984) of the S Lebombo and Swaziland. However, even these show substantial differences from the Mount Alice dykes for some of the trace elements. The rocks of the SRBF are very variable in composition with initial $^{87}Sr/^{86}Sr$ ranging from 0.704 to 0.711. The single Mount Alice sample analysed for Sr-isotopes is within this range but, given the wide range of the SRBF, such an observation cannot be considered diagnostic.

Implications for geochemical provinciality

All the dolerite dykes of the Falkland Islands are of low-Ti affinities, but we recognise three subdivisions of geochemical type within this broad spectrum. First, the solitary dyke in Lively Island is closely comparable with the widespread Mafika Lisiu magma-type in the Lesotho Formation of the Karoo central area (Marsh *et al.* 1997) and thus is broadly comparable to the rocks of the southern Lebombo (Duncan *et al.* 1984), Dronning Maud Land (Harris *et al.* 1990), and some of the dolerites of Coats Land (Brewer *et al.* 1992), though those anxious to emphasize differences between these respective groups may quibble with this statement. This is indeed a fairly variable group, but we would emphasise that mostly these rocks have only slightly elevated initial $^{87}Sr/^{86}Sr$, coupled with low-Ti and often slightly elevated SiO_2.

Second, the N–S dykes are in many respects comparable to the Ferrar magma type, although they have distinctly different Pb isotope ratios which show more affinity with Karoo low-Ti basalts (Marsh *et al.* 1992; 1993).

Third, the E–W dykes, apparently of asthenospheric derivation, are comparable to the dolerites of the Rooi Rand in the southern Lebombo (Armstrong *et al.* 1984). The islands thus appear to lie in a transitional zone, in which there is a geographical overlap of a number of geochemical types. In this respect the area is similar to Coats Land (Brewer *et al.* 1992) where typical Ferrar-type dolerites and Dronning Maud Land dolerite types (equivalent to the low-Ti dolerites of the Karoo Central Area) are both present. Another example of geographical overlap, although in this case between low-Ti and high-Ti basalt types, is the Springbok Flats (Transvaal) area of the Karoo Province (Marsh *et al.* 1997).

In studies of Gondwanaland continental flood basalts, many authors have concluded that geochemical provinciality reflects contributions to basalt source material from different pre-existing lithospheric provinces (although clearly, the dykes derived predominantly from the asthenosphere should be omitted from such discussion). Lithospheric provinces, in both mantle and crust, are unlikely to have sharp boundaries at depth, and surface eruptives and intrusives cannot be relied upon always to remain vertically above their source areas. Thus, a blurring of provincial boundaries, involving spatial overlap of more than one geochemical type is to be expected. In locating provincial boundaries, transitional areas such as the Falkland Islands, Coats Land and the Springbok Flats assume great significance. However-lacking in spatial resolution such observations may be, they are nevertheless highly useful at the scale of Gondwanaland.

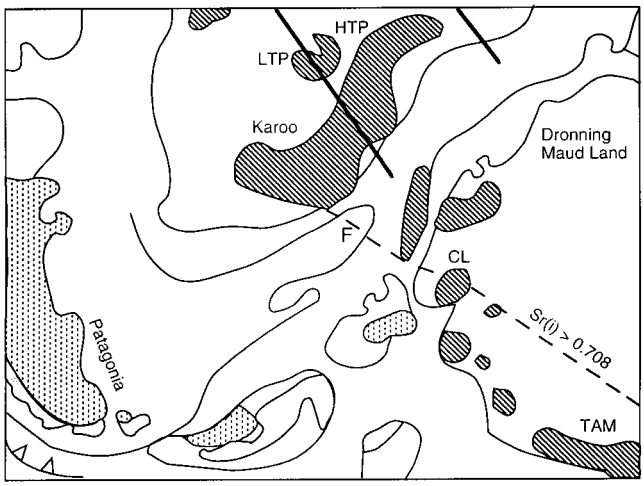

Fig. 9. Geochemical provinces, modified after Elliot (1992). Diagonal stripe ornament, Jurassic basic rocks; vertical dashed ornament, Jurassic silicic rocks; grey shading, magmatic arc; line with triangles, subduction zone. Localities: F, pre-drift position of Falkland Islands; CL, Coats Land; TAM, Transantarctic Mountains. Heavy lines across Africa separate the high-Ti–P (HTP) from low-Ti–P (LTP) provinces. Elliot's boundary marking the limit of the Ferrar Province (Sri>0.708) extends from Coats Land towards the bottom right hand corner of the figure. The extension proposed in the present work runs from Coats Land to the Karoo basin via the Falklands Islands.

In Fig. 9 we give a simplified sketch version of part of Elliot's province map (Elliot 1992, fig. 9). In our version we extend the boundary drawn by Elliot (originally marked as Sr_i>0.7085, here simply as >0.708) to define the northern limit (African reference frame—southern limit in the Antarctic reference frame) of the Ferrar Province within Antarctica. It seems that the only available datum to mark the boundary at that time was Coats Land, and that the strike chosen for the boundary (beneath the ice cap) was intuitive. Our extension takes the boundary from Coats Land, through the pre-drift position of the Falkland Islands into the SE corner of the Karoo basin (to accommodate the Kraai River type), and at least over this relatively short distance, suggests that Elliot's chosen strike is more-than-likely, and, as he supposed, parallel to the subducting margin of Gondwanaland.

Finally, we note again that the Pb isotope compositions of the N–S dykes are substantially different from those of the Ferrar dolerites in Antarctica, despite the extreme similarity of these groups in other respects, including Sr isotope ratios. This suggests the existence of a more complex geochemical provinciality than previously established.

Keith Cox prepared the original version of this paper, but with characteristic generosity and magnanimity chose the order of co-authorship as it appears. Keith died while this paper was in

review and any errors or flaws in the final version are wholly the responsibility of C.M. and R.M.E. G. Taylor is thanked for donation of Cape Orford and Mount Alice samples. N. Charnley, R. Goodwin and K. Parrish (Oxford) and A. Kelly and V. Gallagher (SURRC) are thanked for technical assistance. Laboratory and field work was supported by NERC and the Royal Society. Additional support for isotope research at SURRC was provided by the Scottish Universities Consortium. J. S. Marsh and an anonymous referee are thanked for constructive reviews which greatly improved the paper.

References

Adie, R.J. 1952. The position of the Falkland Islands in a reconstruction of Gondwanaland. *Geological Magazine,* **89,** 401–410.

Armstrong, R.A., Bristow, J.W. & Cox, K.G. 1984. The Rooi Rand dyke swarm, southern Lebombo. *In:* Erlank, A.J. (ed.) *Petrogenesis of the volcanic rocks of the Karoo province.* Geological Society of South Africa Special Publications, **13,** 77–86.

Brewer, T.S., Hergt, J.M., Hawkesworth, C.J., Rex, D. & Storey, B.C. 1992. Coats Land dolerites and the generation of Antarctic continental flood basalts. *In*: Storey , B.C., Alabaster, T. & Pankhurst, R.S. (eds) *Magmatism and the Causes of Continental Break-up*. Geological Society, London, Special Publications, **68,** 185–208.

Bristow, J.W. 1984. Picritic rocks of the North Lebombo and south-east Zimbabwe. *In:* Erlank, A.J. (ed.) *Petrogenesis of the volcanic rocks of the Karoo province.* Geological Society of South Africa Special Publications, **13,** 105–123.

Bristow, J.W., Allsopp, H.L., Erlank, A.J., Marsh, J.S. & Armstrong, R.A. 1984. Strontium isotope characterisation of Karoo volcanic rocks. *In:* Erlank, A.J. (ed.) *Petrogenesis of the volcanic rocks of the Karoo province.* Geological Society of South Africa Special Publications, **13,** 295–329.

Brown, J.W. 1967. Jurassic dolerites from the Falkland Islands and Dronning Maud Land. *British Antarctic Survey Bulletin,* **13,** 89–92.

Carlson, R.W. 1984. Isotopic constraints on Columbia River flood basalt genesis and the nature of the subcontinental mantle. *Geochimica et Cosmochimica Acta,* **48,** 2357–2372.

Cingolani, C.A. & Varela, R. 1976. Investigaciones geologicas y geochronologicas en el extremo sur de la isla Gran Malvina, sector de Cabo Belgrano (Cabo Meredith), Islas Malvinas. *In*: *Actas 6 Congreso Geologico Argentino, Buenos Aires*, 457–473.

Cox, K.G. & Bristow, J.W. 1984. The Sabie River Basalt Formation of the Lebombo Monocline and south-east Zimbabwe. *In:* Erlank, A.J. (ed.) *Petrogenesis of the volcanic rocks of the Karoo province.* Geological Society of South Africa Special Publications, **13,** 125–147.

—— & Hawkesworth, C.J. 1984. Relative contribution of crust and mantle to flood basalt volcanism, Mahabaleshwar area, Deccan Traps. *Philosophical Transactions of the Royal Society of London,* **A310,** 627–641.

Duncan, A.R., Armstrong, R.A., Erlank, A.J., Marsh, J.S. & Watkins, R.T. 1990. MORB-related dolerites associated with the final phase of Karoo basalt vulcanism in southern Africa. *In*: Parker, A.J., Rickwood, P.C. & Tucker, D.H. (eds) *Mafic dykes and emplacement mechanisms*. Balkema, Rotterdam, 119–129.

——, Erlank, A.J. & Marsh, J.S. 1984. Regional geochemistry of the Karoo Igneous Province. *In:* Erlank, A.J. (ed.) *Petrogenesis of the volcanic rocks of the Karoo province.* Geological Society of South Africa Special Publications, **13,** 355–388.

Ellam, R.M. & Cox, K.G. 1991. An interpretation of Karoo picrite basalts in terms of interaction between asthenospheric magmas and the mantle lithosphere. *Earth and Planetary Science Letters,* **105,** 330–342.

Elliot, D.H. 1992. Jurassic magmatism and tectonism associated with Gondwanaland break-up: an Antarctic perspective. *In*: Storey, B.C., Alabaster, T. & Pankhurst, R.S. (eds) *Magmatism and the Causes of Continental Break-up*. Geological Society, London, Special Publications, **68,** 165–184.

Fitch, F.J. & Miller, J.A. 1984. Dating Karoo igneous rocks by the conventional K-Ar and $^{40}Ar/^{39}Ar$ age spectrum methods. *In:* Erlank, A.J. (ed.) *Petrogenesis of the volcanic rocks of the Karoo province.* Geological Society of South Africa Special Publications, **13,** 247–256.

Greenway, M.E. 1972. *The geology of the Falkland Islands*. British Antarctic Survey Scientific Report **76**.

Harris, C., Marsh, J.S., Duncan, A.R. & Erlank, A.J. 1990. The petrogenesis of the Kirwan basalts of Dronning Maud Land, Antarctica. *Journal of Petrology,* **31,** 341–169.

Hart, S.R. 1984. A large-scale isotope anomaly in the Southern Hemisphere mantle. *Nature,* **309,** 753–757.

Hawkesworth, C.J., Mantovani, M.S.M., Taylor, P.N. & Palacz, Z. 1986. Evidence from the Parana of south Brazil for a continental contribution to Dupal basalts. *Nature,* **322,** 356–359.

——, Marsh, J.S., Duncan, A.R., Erlank, A.J. & Norry, M.J. 1984. The role of continental lithosphere in the generation of the Karoo volcanic rocks. *In:* Erlank, A.J. (ed.) *Petrogenesis of the volcanic rocks of the Karoo province.* Geological Society of South Africa Special Publication, **13,** 341–354.

Hergt, J.M., Chappell, B.W., McCulloch, M.T., McDougall, I. & Chivas, A.R. 1989. Geochemical and isotopic constraints on the origin of the Jurassic dolerites of Tasmania. *Journal of Petrology,* **30,** 841–883.

——, Peate, D.W. & Hawkesworth, C.J. 1991. The petrogenesis of Mesozoic Gondwana low-Ti flood basalts. *Earth and Planetary Science Letters,* **105,** 134–148.

Hirose, K. & Kushiro, I. 1993. Partial melting of dry peridotites at high pressures: determination of composition of melts segregated from peridotite using aggregates of diamonds. *Earth and Planetary Science Letters,* **114,** 477–489.

Kushiro, I. 1996. Partial melting of a fertile mantle peridotite at high pressures: an experimental study using aggregates of diamonds. *In:* Basu, A. & Hart, S.R. (eds.) *Earth Processes: reading the isotopic code.* AGU Geophysical Monograph, **95,** 109–122.

Marsh, J.S. & Eales, H.V. 1984. The chemistry and petrogenesis of igneous rocks of the Karoo central area, southern Africa. *In:* Erlank, A.J. (ed.) *Petrogenesis of the volcanic rocks of the Karoo province.* Geological Society of South Africa Special Publications, **13,** 27–67.

——, Armstrong, R.A. & Sweeney, R.J. 1993. Pb-Nd-Sr isotopes and the identification of mantle and crustal components in Karoo mafic volcanic rocks. *In*: *IAVCEI General Assembly, Canberra Abstract Volume* 68.

——, Hooper, P.R., Rehacek, J., Duncan, R.A. & Duncan, A.R. 1997. Stratigraphy and age of Karoo basalts of Lesotho and implications for correlations within the Karoo Igneous Province. *In:* Mahoney, J.J. & Coffin, M.F. (eds.) *Large igneous provinces: continental, oceanic and planetary flood volcanism.* AGU Geophysical Monographs, **100,** 247–272.

——, Sweeney, R.J. & Armstrong, R.A. 1992. New Pb, Sr and Nd isotope data from the Karoo province. *Geological Society of South Africa 24th Congress*, Bloemfontein, Abstract.

Melluso, L., Beccaluva, L., Brotzu, P., Gregnanin, A., Gupta, A.K., Morbidelli, L. & Traversa, G. 1995. Constraints on the mantle sources of the Deccan Traps from the petrology and geochemistry of the basalts of Gujarat State (western India). *Journal of Petrology,* **36,** 1393–1432.

Menzies, M.A., Leeman, W.P. & Hawkesworth, C.J. 1984. Geochemical and isotopic evidence for the origin of continental flood basalts with particular reference to the Snake River Plain, Idaho, U.S.A. *Philosophical Transactions of the Royal Society of London,* **A310,** 643–660.

Mitchell, C., Taylor, G.K. & Cox, K.G. 1986. Are the Falkland Islands a rotated microplate? *Nature,* **319,** 131–134.

Molzahn, M., Reisberg, L. & Wörner, G. 1996. Os, Sr, Nd, Pb, O isotope and trace element data for the Ferrar flood basalts, Antarctica: evidence for an enriched subcontinental lithospheric source. *Earth and Planetary Science Letters,* **144,** 529–546.

Mussett, A.E. & Taylor, G.K. 1994. ^{40}Ar-^{39}Ar ages for dykes from the Falkland Islands with implications for the break-up of southern Gondwanaland. *Journal of the Geological Society, London,* **151,** 79–81.

Peate, D.W. 1991. *Stratigraphy and petrogenesis of the Paraná continental flood basalts, southern Brazil*. PhD thesis, The Open University unpublished.

—— & Hawkesworth, C.J. 1996. Lithospheric to asthenospheric transition in low-Ti flood basalts from southern Paraná, Brazil. *Chemical Geology,* **127,** 1–24.

Richardson, S.H., Erlank, A.J., Duncan, A.R. & Reid, D.L. 1982. Correlated Nd, Sr and Pb isotope variation in Walvis Ridge basalts and implications for the evolution of their mantle source. *Earth and Planetary Science Letters,* **59,** 327–342.

Roeder, P.L. & Emslie, R.F. 1970. Olivine-liquid equilibria. *Contributions to Mineralogy and Petrology,* **29,** 275–289.

Rollinson, H.R. 1993. *Using geochemical data: evaluation, presentation, interpretation*. Longman Group UK, Harlow.

Scarrow, J.H. & Cox, K.G. 1995. Basalts generated by decompressive melting of a mantle plume: a case study from the Isle of Skye, NW Scotland. *Journal of Petrology,* **36,** 3–22.

Siders, M.A. & Elliot, D.H. 1985. Major and trace element geochemistry of the Kirkpatrick Basalt, Mesa Range, Antarctica. *Earth and Planetary Science Letters,* **72,** 54–64.

TAYLOR, G.K. & SHAW, J. 1989. The Falkland Islands; new palaeomagnetic data and their origin as a displaced terrane from Southern Africa. *In:* HILLHOUSE, J.W. (ed.) *Deep structure and past kinematics of accreted terranes (IUGG Volume 5).* AGU Geophysical Monographs, **50,** 59–72.

WRIGHT, T.L. & DOHERTY, P.C. 1970. A linear programming and least squares computer method for solving petrologic mixing problems. *Geological Society of America Bulletin,* **81,** 1995–2008.

Received 1 May 1998; revised typescript accepted 10 January 1999.
Scientific editing by Hugh Rollinson.